Dynamical structure factor $S(\vec{Q}, \omega)$ of rare-gas solids

Jean Pierre Hansen
Laboratoire de Physique Théorique des Liquides, Université Paris VI, 75230 Paris, France*

Michael L. Klein
Chemistry Division, National Research Council of Canada, Ottawa, Canada K1A 0R6

(Received 26 September 1973; revised manuscript received 5 August 1975)

The classical molecular-dynamics (MD) method was used to make a systematic study of the dynamical structure factor $S(\vec{Q}, \omega)$ for systems of N particles disposed on an fcc lattice with periodic boundary conditions and interacting with n shells of neighbors via a Mie–Lennard-Jones (12-6) potential. Calculations were carried out for $N(n) = 108(3)$, 256(3 or 5), 864(3), and 2048(1) at reduced densities and temperatures corresponding to roughly the melting point of the model and one-half this temperature. Phonons of a particular wave vector $\vec{Q}$ were identified by the peaks in $S(\vec{Q}, \omega)$. The one-phonon approximation to $S(\vec{Q}, \omega)$ was investigated, as was the $\vec{Q}$ dependence of certain phonons. The temperature shifts of phonons for both constant density and pressure were studied along with their shifts with density at constant temperature. The one-phonon $S(\vec{Q}, \omega)$ for certain zone-boundary phonons is compared with the predictions of a self-consistent phonon approximation that includes phonon damping. Even at half the melting temperature the latter theory is not totally adequate and possible reasons for this are discussed. Finally, as a by-product of the MD calculations, certain equilibrium properties were also obtained and compared with perturbation-theory results that use hard spheres as a reference system. Results of the latter procedure were very poor.

I. INTRODUCTION

The molecular-dynamics (MD) method, as developed for hard-sphere systems by Alder and Wainwright[1] and for continuous potentials by Rahman[2] and Verlet[3] has been extensively used to simulate the equilibrium and time-dependent properties of a wide variety of liquids and dense fluids. The related Monte Carlo method developed by Metropolis *et al.*[4] and by Wood[5] has also been widely applied to the study of equilibrium (or static) properties of liquids and of solids. In particular the elastic constants of rare-gas solids have been computed in this way[6] and compared to the predictions of self-consistent-phonon theories including anharmonic corrections.[7] However, the dynamical properties of solids can only be simulated by the molecular-dynamics method and one aim of the present work was to provide a test of the self-consistent-phonon theory dynamical properties in rare-gas solids over a wide range of temperatures. The only previous computer simulation of the lattice dynamics of rare-gas solids[8] was restricted to the computation of self-correlation functions and to an indirect determination of phonon dispersion curves from the response of a crystal to external disturbances. However, lattice vibrations are highly collective modes directly related to the spectrum of the density fluctuations which in turn are related to the differential cross section for coherent inelastically scattered thermal neutrons. This spectrum is the dynamical structure factor $S(\vec{Q}, \omega)$, the Fourier transform with respect to time of the correlation function of the density operator

$$\rho_{\vec{Q}}(t) = \sum_{i=1}^{N} e^{i\vec{Q}\cdot\vec{r}_i(t)} , \tag{1}$$

where the sum is over the N atoms of the system, and

$$S(\vec{Q}, \omega) = \int_{-\infty}^{+\infty} e^{i\omega t} F(\vec{Q}, t)\, dt , \tag{2}$$

$$F(\vec{Q}, t) = (1/N)\langle \rho_{\vec{Q}}(t)\rho_{-\vec{Q}}(0)\rangle , \tag{3}$$

where the angular brackets denote statistical average; $F(\vec{Q}, t)$ is frequently referred to as the "intermediate scattering function" and can be calculated "exactly" by the MD method for systems of several hundred atoms. The first calculation of this type was made by Levesque *et al.*[9] for rare-gas liquids near the triple point. Since then the dynamical structure factor has been computed for a variety of fluid or liquid systems, including liquid metals[10] and the classical one-component plasma.[11] In the present work we apply essentially the same technique to the case of crystalline rare gases. A brief preliminary report of parts of this work was presented elsewhere.[12] Extensions to the case of solid alkali halides, solid nitrogen, and solid alkalis will be published elsewhere.[13]

The recent availability of experimental data on inelastic neutron scattering from rare-gas single crystals at high temperatures[14] renders the present work particularly timely. In fact, to allow a direct comparison between experiment and computer simulation, several calculations were made for wave vectors and under density-temperature conditions very close to some of the experimental conditions. The simulation of dynamical proper-

ties of solids at high temperatures is also relevant for quantitative comparison with the recent experimental spectra of depolarized light scattering from rare gas crystals,[15] as has been done recently for simple liquids.[16] That part of the work will be presented separately.[17] Here we restrict ourselves to a presentation and discussion of the $S(\vec{Q}, \omega)$ data.

The paper is organized as follows: Technical details of our calculations are presented in Sec. II. Section III deals with the equilibrium properties which have been obtained as a byproduct of the MD computations. The results are compared to the predictions of the thermodynamic perturbation theory.[18] The $S(\vec{Q}, \omega)$ data are presented in Sec. IV and compared with available experimental results. Section V is devoted to a confrontation of our results with the prediction of self-consistent-phonon theory. Some concluding remarks are contained in Sec. VI.

II. COMPUTATION

In the usual manner, the time evolution of a system of N atoms was determined over a certain time interval τ, by solving numerically Newton's equations of motions for the N atoms using Verlet's finite difference algorithm.[3] The usual periodic boundary conditions were assumed and the N atoms interacted through the standard Mie–Lennard-Jones two-body potential

$$v(r) = 4\epsilon[(\sigma/r)^{12} - (\sigma/r)^{6}] \,. \tag{4}$$

This potential was used, rather than more "realistic" potentials, because it yields satisfactory results for the dense rare-gas liquids and because it has been widely used in the self-consistent-phonon calculations. Moreover, the results expressed in "reduced units," i.e., with σ, ϵ, and $\tau_0 = (m\sigma^2/48\epsilon)^{1/2}$ chosen as length, energy, and time units, can be easily converted to absolute units for any one of the rare gases, by an appropriate choice of the potential parameters ϵ and σ. Our energy unit τ_0^{-1} corresponds roughly to about 18 cm^{-1}, 0.54 THz, or 2.23 meV for ^{36}Ar, if one uses $\sigma = 3.405$ Å and $\epsilon/k = 119.8$ K.

Runs were made in the reduced temperature range $0.28 \leq T^* = kT/\epsilon \leq 1.2$ and in the reduced density range $0.97 \leq \rho^* = N\sigma^3/V \leq 1.031$, for systems of 108, 256, 864, and 2048 atoms. We recall that the triple point of a Lennard-Jones system corresponds to $T^* \simeq 0.68$ and $\rho^*_{\text{solid}} \simeq 0.96$.[19] In each run the initial configuration was chosen to be a perfect fcc lattice and we used a time increment of $0.032\tau_0$ in the finite difference algorithm; this corresponds to $\sim 10^{-14}$ sec for argon. The integration of the equations of motion was carried out for up to 40 000 time steps in each run; consequently τ, the total time interval, was of the order of 4.10^{-10} sec for argon. Fourteen independent runs were made, some of them under very similar $\rho^* - T^*$ conditions, but for different N, in order to study the N dependence of various quantities.

In the various runs, each of the N atoms was made to interact with a fixed number of shells of neighbors n. The contribution of the remaining shells to the thermodynamic properties (e.g., the equation of state) was accounted for by adding static lattice sum corrections. Because the rms displacement of the atoms from their lattice sites is only a small fraction of the lattice parameter (of the order of 14% at melting[20]) this procedure introduces negligible errors for $n \geq 3$. For $N = 108$, 256, and 864, n was chosen equal to 3 or 5 (42 or 78 neighbors); however, for the largest system ($N = 2048$), n was taken equal to 1 (12 neighbors) in order to stay within reasonable limits for the computer time (which is proportional to $N \times n$).

It should be stressed that the MD calculations are purely classical and ignore all quantum effects. In the temperature range considered here, this is justified for the heavier rare gases. Their contribution to the equilibrium properties (in particular to the Helmholtz free energy) can be estimated by calculating the h^2 term of the Wigner expansion[21]; this expansion has been shown to be strongly convergent even in the vicinity of the triple point of neon[22] and will be used in Sec. III. The most important result of the present work is the computation of the dynamical structure factor (2), as a function of ω, for several $\vec{Q}$ vectors.

The dynamical structure factor $S(\vec{Q}, \omega)$ can be computed in either of two ways. The first method consists in computing the intermediate scattering function (3) by correlating the real and imaginary parts of the density operator (1) at different times and finally taking the Fourier transform (2). Typical $F(\vec{Q}, t)$ are reproduced in Fig. 1 for two $|\vec{Q}|$ values (two different phonons) along the [100] direction. Figure 2 shows the corresponding $S(\vec{Q}, \omega)$. The difficulties of this method are at once apparent from Fig. 1: for low-$|\vec{Q}|$ phonons, the correlation function decays very slowly (long lifetime) and one has to numerically autocorrelate the density operator over a long time interval in order not to introduce significant truncation errors.

The second method has been described in Ref. 12 and consists in computing directly (in the course of the MD run) the Fourier-Laplace transform $\rho_{\vec{Q}}(\omega)$ of the density operator, using the formula

$$S(\vec{Q}, \omega) = \frac{1}{N} \int_{-\infty}^{+\infty} e^{i\omega t} \langle \rho_{\vec{Q}}(t) \rho_{-\vec{Q}}(0) \rangle \, dt$$

$$= \lim_{\tau \to \infty} \int_0^{\tau} e^{i\omega t} \rho_{\vec{Q}}(t) \, dt \int_0^{\tau} e^{-i\omega t'} \rho_{-\vec{Q}}(t') \, dt'$$

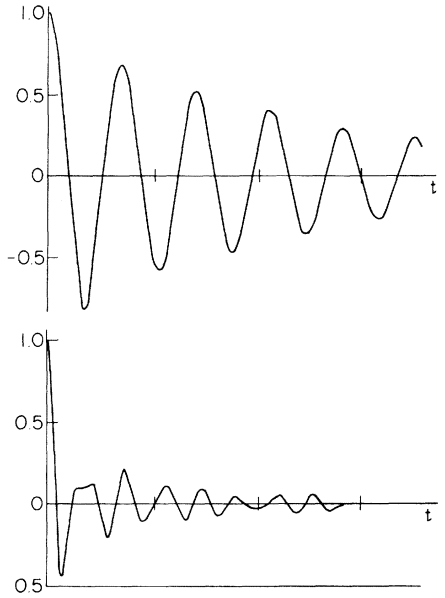

FIG. 1. "Intermediate scattering function" $F(\vec{Q}, t)$, for two $\vec{Q}$ values whose Fourier transforms are shown in Fig. 2. The increment on the time scale corresponds to $6.4\tau_0$ units.

$$S(\vec{Q}, w) = \frac{1}{N} \lim_{\tau \to \infty} |\rho_{\vec{Q}}(\omega)|^2 .$$

For MD calculations running over 20 000–40 000 time steps, the truncation error is negligible, but the disadvantage of this method is that the statistical "noise" is more difficult to eliminate, because it is automatically included in the Fourier-Laplace transform. In view of this statistical noise, we convoluted the raw data with a Gaussian width function which usually had a full width at half-maximum (FWHM) $= 0.1\tau_0^{-1}$. This is essentially equivalent to truncating $F(\vec{Q}, t)$ at $t \simeq 40\pi\tau_0$ (approximately 4000 time steps). Comparing the results obtained by the two methods, they appear to yield very similar $S(\vec{Q}, \omega)$. The second method is slightly more convenient and was used in most of the work.

The appearance of the scalar product $\vec{Q} \cdot \vec{r}$ in the density operator (1) allows only longitudinal response to be observable in symmetry directions, such as $[00\zeta]$; this situation is the same as in isotropic fluids. However, the transverse response can be observed for $\vec{Q}$ vectors that have nonzero reciprocal-lattice vectors $\vec{K}$, i.e., outside the first Brillouin zone.

In the classical limit, $S(\vec{Q}, \omega)$ is even in ω. However, if quantum effects are duly taken into account, the well-known detailed balance condition

$$S(\vec{Q}, -\omega) = e^{-\beta\hbar\omega} S(\vec{Q}, \omega) \tag{5}$$

implies the presence of odd terms in $S(\vec{Q}, \omega)$; consequently, the intermediate scattering function (3) has an imaginary part in the quantum case (which is a direct consequence of the fact that the atom positions at different times do not commute). This imaginary part can be calculated to first order in $\hbar$ from the classical (real) intermediate scattering function.[23] However, this procedure has not been applied. This point is discussed further in Sec. V when we compare our MD calculations with self-consistent-phonon calculations.

III. EQUILIBRIUM PROPERTIES

The MD method yields equilibrium as well as dynamical properties; we first discuss our results for the equilibrium properties. We have computed the following thermodynamic quantities (a) the excess internal energy per particle

$$\frac{U}{N} = \frac{1}{N} \left\langle \sum_{i<j} v(r_{ij}) \right\rangle , \tag{6}$$

(b) the equation of state, calculated from the virial theorem

$$Z = \frac{P}{\rho kT} = 1 - \frac{1}{3NkT} \left\langle \sum_{i<j} r_{ij} \frac{dv(r_{ij})}{dr_{ij}} \right\rangle , \tag{7}$$

and (c) the specific heat at constant volume (per particle) which, in the microcanonical ensemble, can be calculated from the fluctuation of the temperature[24]

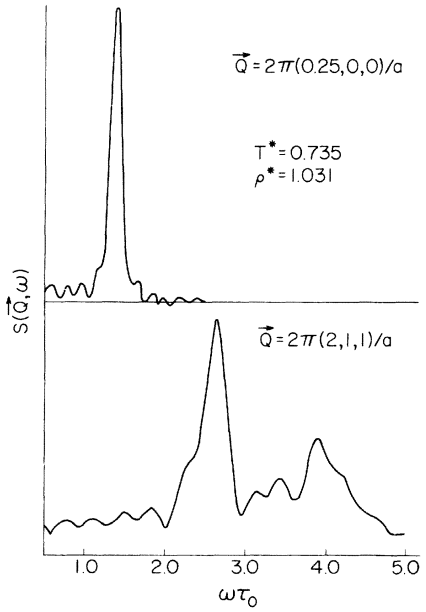

FIG. 2. Two typical $S(\vec{Q}, \omega)$ curves taken from run No. 13 of Table I. The upper curve shows the longitudinal phonon while the lower one shows both the transverse and longitudinal zone-boundary phonons in the $[\zeta 00]$ direction.

TABLE I. Summary of equilibrium properties determined in the MD runs and comparison of selected quantities with a perturbation theory that uses a hard-sphere reference system.

Run	N	n	T^*	ρ^*	$10^2\langle u^{*2}\rangle$	Z	$Z^{\text{pert.}}$	$\frac{U}{N}$	$\frac{C_v}{Nk}$	$\frac{\langle \Delta V^*\rangle}{24}$	$\frac{F^{\text{pert.}}}{NkT}$	$\frac{F^{(1)}}{NkT}$ (Ne)
1	256	5	0.2814	1.031	0.477	−2.933	−1.386	−8.106	1.61	40.75	−22.36	4.66
2	108	3	0.3185	1.031	0.494	−1.604	8.16	−8.058	1.74	41.82	−19.11	3.67
3	256	5	0.319	1.031	0.535	−1.600	8.21	−8.055	1.78	41.73	−19.07	3.67
4	864	3	0.321	1.031	0.556	−1.595	8.47	−8.054	1.74	41.90	−18.92	3.64
5	2048	1	0.3375	1.030	0.564							
6	864	3	0.501	1.003	1.013	−0.407	−0.762	−7.710	1.95	41.12	−10.42	1.468
7	864	3	0.504	1.003	1.056	−0.354	−0.732	−7.706	1.95	41.20	−10.33	1.453
8	864	3	0.6364	0.98	1.496	0.100	0.460	−7.429	2.11	40.55	−7.20	0.897
9	864	3	0.647	0.98	1.522	0.227	0.656	−7.416	2.10	40.81	−7.01	0.872
10	2048	1	0.726	0.97	1.662							
11	864	3	0.7326	0.97	1.864	0.693	1.406	−7.255	2.34	41.32	−5.72	0.690
12	864	3	0.735	0.97		0.714	1.443	−7.252	2.28	41.37	−5.68	0.686
13	256	3	0.735	1.031	1.200	3.816	4.141	−7.505	2.33	42.21	−5.52	0.866
14	256	3	1.197	1.031	1.983	5.274	6.294	−6.916	2.87	63.26	−1.76	0.396

$$\frac{C_v}{Nk} = \frac{3}{2[1-(3/2\rho^*T^*)][\langle T^{*2}\rangle - \langle T^*\rangle^2]} . \tag{8}$$

As is well known, the MD and Monte Carlo methods do not readily yield the Helmholtz free energy (or alternatively the entropy) directly, but this can be calculated by integrating numerically the equation of state[25]; in this way the Helmholtz free energy for rare-gas solids was computed for several isotherms above the triple point,[19] but because the primary aim of the present work is the study of the dynamical properties of rare gas solids we have not attempted to perform the similar computations in the $\rho^* - T^*$ range considered here. We have however calculated the Helmholtz free energy per particle F/NkT, using thermodynamic perturbation theory based on a hard-sphere reference system.[18] This theory yields reasonable results in the triple-point region.[18] We have also calculated the equation of state using perturbation theory and compared it to our "exact" results in Table I listing the various equilibrium properties which we have obtained.

The first quantum correction to the Helmholtz free energy is given by[21,22]

$$F^{(1)}/NkT = \tfrac{1}{24}\langle \Delta V^*\rangle(\Lambda/T^*)^2 , \tag{9}$$

where

$$\langle \Delta V^*\rangle = \frac{1}{N\epsilon}\left\langle \sum_{i=1}^{N} \nabla_i^2 \left(\sum_{i<j} v(r_{ij}) \right) \right\rangle$$

is the average of the Laplacian of the total potential energy expressed in reduced units, and $\Lambda^2 = \hbar^2/\sigma^2 m\epsilon$ is the dimensionless de Boer quantum parameter. For neon $\Lambda^2 \sim 0.896\times10^{-2}$ if one uses $\sigma = 2.74$ Å and $\epsilon/k = 35.6$ K and for argon, $\Lambda^2 \sim 0.874\times10^{-3}$ if one uses $\sigma = 3.405$ Å and $\epsilon/k = 119.8$ K. Thus the first-order quantum correction is seen to be ten times smaller for argon than for neon at the same $\rho^* - T^*$ and it is even smaller for the heavier rare gases Kr and Xe. In Table I we list the values obtained for $\frac{1}{24}\langle \Delta V^*\rangle$ as well as the corresponding values of $F^{(1)}/NkT$ in the case of Ne. Comparing this to the classical free energy obtained from perturbation theory, it is seen that in the $\rho^* - T^*$ range considered in this work the quantum corrections to the free energy are rather large for neon but they are only about 2% for argon.

Finally, we have computed the mean-square displacement of an atom from its lattice site

$$\langle u^2\rangle = \frac{1}{N}\left\langle \sum_i u_i^2 \right\rangle , \tag{10}$$

where $\vec{u}_i = \vec{r}_i - \vec{R}_i$ is the displacement and $\vec{R}_i$ is the lattice site of the ith atom. The results for $\langle u^2\rangle$ are listed in Table I along with the thermodynamic properties. The strong N dependence of $\langle u^2\rangle$ is quite apparent by comparing the results in run Nos. 2, 3, and 4; $\langle u^2\rangle$ increases with N, in agreement with the predictions of harmonic theory. On the other hand the N dependence of the equation of state and internal energy appears to be negligible. Note that the relative statistical error on Z, $\langle u^2\rangle$ and U/NkT is less than 1%, but of the order of 5% for C_v/Nk. In the case of the 2048-particle system, the thermodynamic properties are not listed because, as we have explained in Sec. II, the corresponding runs were made for interactions with one shell of neighbors only.

Comparison of the "exact" equation-of-state results and the predictions of the perturbation theory clearly shows the inadequacy of a perturbation theory of the solid based on a hard-sphere reference system, especially at low temperatures. This was already emphasized in Ref. 18; the predicted free energies agree within a few percent

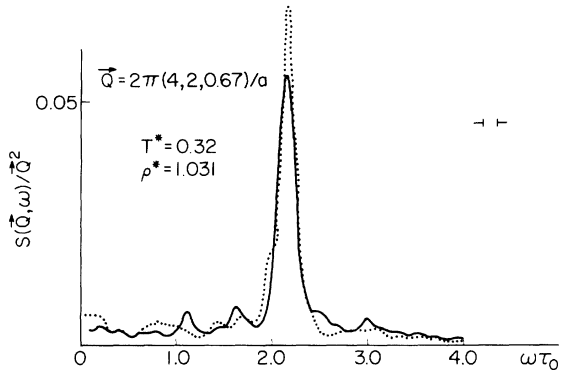

FIG. 3. Dependence of $S(\vec{Q},\omega)$ on the system size. The solid curve is taken from run No. 2 (108 particles) while the dotted curve is from run No. 4 (864 particles).

with the computer results in the triple point region, but at lower and higher temperatures the agreement becomes rapidly worse. The equation-of-state results, obtained by differentiating the free energy, are not surprisingly even poorer and the data listed in Table I clearly illustrate the complete failure of the theory at low temperatures. This is in marked contrast with the situation in the fluid, where the perturbation theory works remarkably well.[26] The fundamental reason seems to lie in the inadequacy of the completely anharmonic hard-sphere reference system. In Ref. 17 it is also shown that the hard-sphere solid is completely inadequate to describe the dynamics of rare-gas crystals, as probed by depolarized light scattering.

IV. DYNAMICAL STRUCTURE FACTOR

For each of the 14 runs listed in Table I, $S(\vec{Q},\omega)$ has been computed for selected wave vectors. Moreover, we calculated the corresponding one-phonon approximation

$$S_1(\vec{Q},\omega)=\frac{e^{-2W}}{N}\lim_{\tau\to\infty}\frac{1}{\tau}\left|\tilde{\rho}_{\vec{Q}}(\omega)\right|^2 , \tag{11}$$

where $\tilde{\rho}_{\vec{Q}}(\omega)$ is the Fourier-Laplace transform of

$$\tilde{\rho}_{\vec{Q}}(t)=\sum_{i=1}^{N} e^{i\vec{Q}\cdot\vec{R}_i}\,\vec{Q}\cdot\vec{u}_i(t) \tag{12}$$

and $2W=\frac{1}{3}|\vec{Q}|^2\langle u^2\rangle$.

Except for large $|\vec{Q}|$, these results are essentially identical with the full $S(\vec{Q},\omega)$. This feature is not unexpected in view of the sum rules which must be satisfied by S and S_1,

$$\frac{1}{2\pi}\int_{-\infty}^{+\infty}\omega^2 S(\vec{Q},\omega)\,d\omega=\frac{kTQ^2}{m} , \tag{13}$$

$$\frac{1}{2\pi}\int_{-\infty}^{+\infty}\omega^2 S(\vec{Q},\omega)\,d\omega=e^{-2W}\frac{kTQ^2}{m} . \tag{14}$$

Except at the lowest $\vec{Q}$ vectors, where the phonon peaks are very sharp, our numerical data satisfy these sum rules to within 10%.

If $\vec{Q}$, ω, and $S(\vec{Q},\omega)$ are expressed in reduced units, (13) can be recast in the form

$$\frac{1}{2\pi}\int_{-\infty}^{+\infty}\omega^{*2}S^*(\vec{Q}^*,\omega^*)\,d\omega^*=\frac{Q^{*2}T^*}{48} . \tag{15}$$

In this form the sum rule will serve as a basis of our qualitative understanding of our results.

A. N dependence

Figure 3 shows $S(\vec{Q},\omega)$ for $\vec{Q}=(2\pi/a)(4,2,\frac{2}{3})$, $T^*=0.32$, $\rho^*=1.031$, computed with systems of $N=108$ and $N=864$ atoms. Within the resolution and statistical uncertainties of our data, the two results are identical. For all other cases where comparisons were possible, peak positions showed no significant N dependence.

B. Dispersion curves

Figures 4(a) and 4(b) show the dispersion curves for the $[00\zeta]$ longitudinal phonons for $T^*=0.34$, $\rho^*=1.030$ and $T^*=0.73$, $\rho^*=0.97$. For $\vec{Q}$ vectors close to the zone boundary, the peaks are seen to broaden substantially, even at $T^*=0.32$, in qualitative agreement with quasiharmonic perturbation theory.[27] As expected the higher T^* phonons are considerably less well defined. This explains why recent neutron scattering experiments were unable to give clear evidence of their existence in solid Kr and Ar near melting.[28,29]

C. Q dependence

In Fig. 5 we show the longitudinal phonon with $\vec{q}=\vec{Q}-\vec{K}=(2\pi/a)(\frac{1}{2},0,0)$, for two reciprocal-lattice vectors, $\vec{K}=(2\pi/a)(0,0,0)$ and $\vec{K}=(2\pi/a)(4,0,0)$ at $T^*=0.337$, $\rho^*=1.030$, and $T^*=0.73$, $\rho^*=0.97$. For easier comparison $S(\vec{Q},\omega)$ for larger $\vec{Q}$ has been divided by the ratio of the squares of the wave vectors. The ratio of the peak height, is close to the ratio of the respective Debye-Waller factors e^{-2W}, as one expects for one-phonon scattering. However, the larger $\vec{Q}$ phonons show enhanced background (multiphonon) scattering. This background contributes a fraction $(e^{2W}-1)$ of the total scattering[30] and is necessarily large when $\langle u^2\rangle$ is large and hence e^{-2W} is small. This phonon appears to have a shoulder on the left of the main peak which grows with T^*. The same phonon but with $\vec{K}=(2,0,0)\,2\pi/a$, has been studied experimentally in ^{36}Ar and exhibits a similar feature.[29] The large frequency shift of the main peak should be noted. Temperature and density shifts of the phonon peaks will now be discussed in more detail.

D. Temperature shifts at constant density

Figure 6 shows the transverse phonon at $\vec{Q}=(2\pi/a)(2,\frac{1}{2},0)$ for a fixed density $\rho^*=1.031$ and

two different temperatures: $T^* = 0.735$ and $T^* = 1.20$; this phonon exhibits a sizable negative shift as T^* increases. Figure 7 shows the longitudinal phonon at $\vec{Q} = (2\pi/a)(\frac{1}{2}, 0, 0)$ under identical temperature and density conditions. This time the shift is small and positive. The apparent increase in intensity as T^* is increased is governed entirely by the sum rule equation (15).

E. Temperature shifts at constant pressure

Figure 8 shows the temperature shifts for transverse phonons propagating in [00ζ] direction for roughly the same $\rho^* - T^*$ states studied experimentally by Batchelder *et al.*[14] As expected the peaks shift to lower frequencies and broaden as T^* increases, and in addition the multiphonon background grows. This behavior is again compatible with the sum rule equation (15).

Figure 9 compares the MD percentage frequency shifts with the experimental results[14,29] and the results of a self-consistent-phonon calculation.[31] The MD results are in better agreement with the experimental data than the phonon calculations.

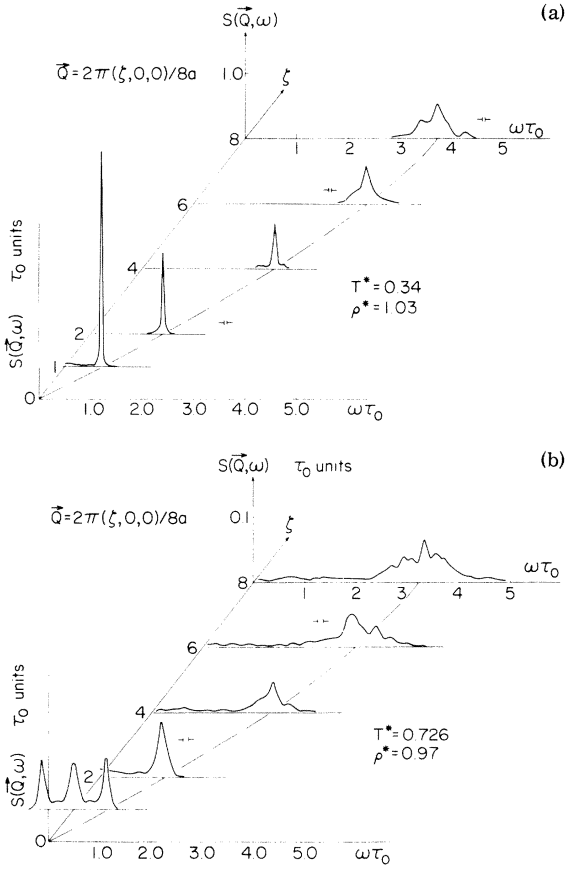

FIG. 4. (a) Dispersion curve for longitudinal phonons propagating in the [00ζ] direction taken from run No. 5. (b) Dispersion curve for longitudinal phonons propagation in the [00ζ] direction taken from run No. 10. Note the Rayleigh-Brillouin triplet for the smallest wave vector.

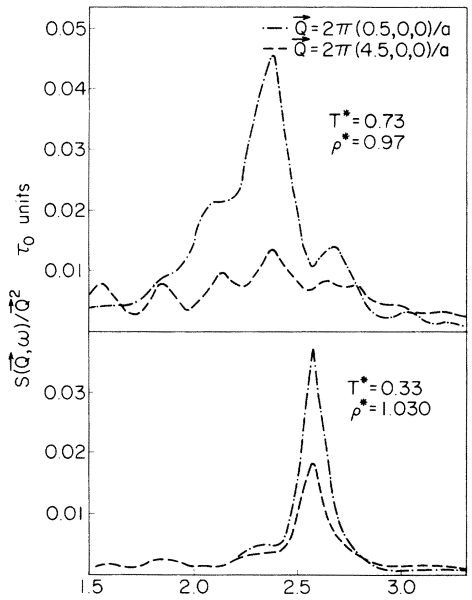

FIG. 5. $\vec{Q}$ dependence of $S(\vec{Q}, \omega)$ for the longitudinal phonon halfway to the zone boundary in the [00ζ] direction. The upper curve corresponds to roughly the triple point of the (12-6) potential while the lower curve corresponds to about one-half the melting point at zero pressure. Data taken from run Nos. 10 and 5, respectively.

F. Density shifts at constant temperature

Returning to Fig. 7 we see the strong negative shift in the longitudinal $(\frac{1}{2}, 0, 0)$ phonon peak position on changing the density from 1.031 to 0.97 at $T^* = 0.735$. The relative shift amounts to about 15% which compares well with predictions using

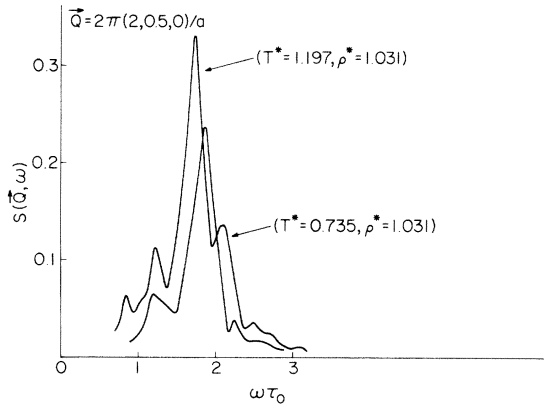

FIG. 6. Temperature dependence of $S(\vec{Q}, \omega)$ at constant density for the transverse phonon halfway to the zone boundary in the [00ζ] direction. Taken from run Nos. 13 and 14.

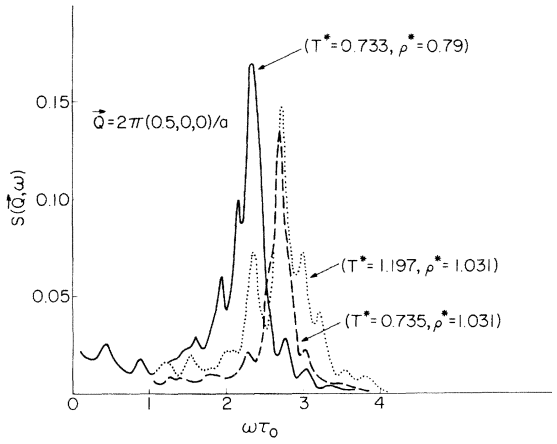

FIG. 7. Temperature dependence at constant density and density dependence at constant temperature of $S(\vec{Q}, \omega)$ for the longitudinal phonon halfway to the zone boundary in the [00ζ] direction. Data taken from run Nos. 13 (dashed) 14 (dots) and 11 (full curve).

the Grüneisen approximation. The increase in intensity accompanying the negative frequency shift is a consequence of the sum rule equation (15).

G. Rayleigh-Brillouin triplet

The lowest $\vec{Q}$ phonon studied was obtained with 2048-particle system and corresponds to $\vec{Q} = (2\pi/a)(\frac{1}{8}, 0, 0)$. This phonon is shown in Fig. 4(b) and clearly exhibits a Rayleigh-Brillouin triplet. From the width of the Rayleigh peak $\Gamma_R = DQ^2$, one can extract an estimate of the thermal diffusivity, which is related to the thermal conductivity by $D = \kappa/\rho C_p$. We find $D \cong 0.1\,\tau_0^{-1}$ which compares favorably with the value derivable from the experimental value of κ for Ar.[32] Less-well-resolved results were obtained with the 864-particle system, for which the smallest allowable $\vec{Q}$ vector is $(2\pi/a)(\frac{1}{6}, 0, 0)$. The Brillouin peak position in the latter case agrees within statistical uncertainties with the sound velocities obtained by the Monte Carlo method[6] for the same system.

V. COMPARISON WITH SELF-CONSISTENT PHONON CALCULATIONS

A. Preamble

Following the work of Maradudin and Fein[33] and Ambegaokar, Conway, and Baym[30] we can write the intermediate scattering function as a power series in $\vec{Q}$:

$$S(\vec{Q}, t) = S_0 + S_1 + S_{\text{int}} + S_2 + \cdots . \tag{16}$$

These terms describe successively the elastic (Bragg) scattering, one-phonon inelastic scattering, the interference between the one-phonon and two-phonon scattering, and the two-phonon inelastic scattering, etc. A detailed expression for S_1 has been given earlier in Eqs. (11) and (12). For a harmonic crystal [either quasiharmonic, or self-consistent harmonic (SCHA)] the appropriate ensemble average occurring in S_1 is readily evaluated and one obtains

$$S_1^0(\vec{Q}, \omega) = \frac{\hbar}{2m} e^{-2W} \sum_{q\lambda} \Delta(\vec{Q} - \vec{q}) \frac{(\vec{Q} \cdot \vec{e}_{q\lambda})^2}{\omega_{q\lambda}} A_{q\lambda}^0(\omega) , \tag{17}$$

$$A_{q\lambda}^0(\omega) = 2\pi[(\bar{n}_{q\lambda} + 1)\delta(\omega - \omega_{q\lambda}) + \bar{n}_{q\lambda}\delta(\omega + \omega_{q\lambda})], \tag{18}$$

where $\omega_{q\lambda}$ and $\vec{e}_{q\lambda}$ are the harmonic phonon frequen-

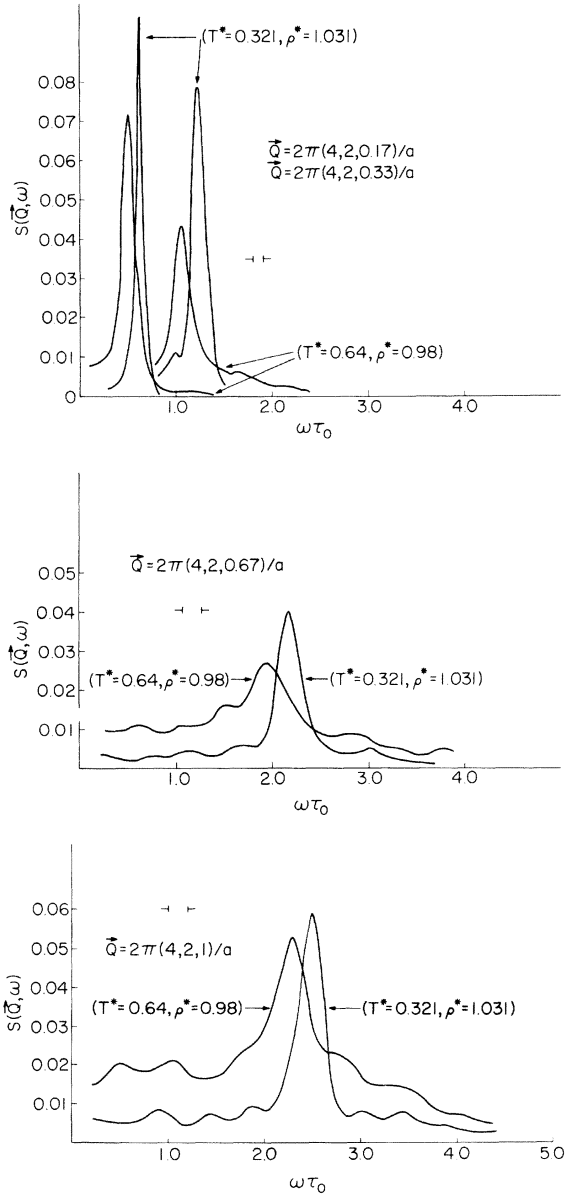

FIG. 8. Temperature dependence of $S(\vec{Q}, \omega)$ at roughly zero pressure. The FWHM of the Gaussian filter function used to smooth the raw $S(\vec{Q}, \omega)$ data is also shown. The data were taken from run Nos. 4, 8, and 9.

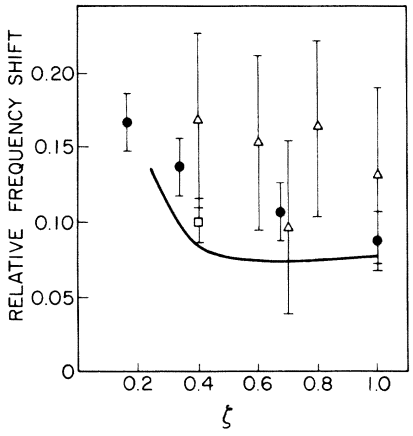

FIG. 9. Relative shift of the peaks in $S(\vec{Q}, \omega)$ taken from Fig. 8 (full circles) compared with experimental data for ^{36}Ar under similar conditions taken from Refs. 29 (open square) and 14 (open triangles). The solid line is taken from self-consistent-phonon calculation of Ref. 31.

cies and eigenvectors and $\bar{n}_{q\lambda}$ is the phonon occupation number. The delta function $\Delta(\vec{Q} - \vec{q})$ indicates that the momentum transfer must be equal to the phonon wave vector plus or minus a reciprocal-lattice vector $\vec{K}$. The superscript 0 denotes the harmonic approximation. $S_1^0(Q, \omega)$ has δ-function peaks at the appropriate phonon frequencies.

In the harmonic approximation S_{int} vanishes while S_2 gives rise to a broad (structured) background extending to twice the maximum frequency.

In an anharmonic crystal the δ-function peaks become broadened and shifted and one can show that (at least for the high-symmetry directions such as [100], [110], and [111] in the fcc lattice)

$$S_1(\vec{Q}, \omega) = \frac{\hbar}{2m} e^{-2W} \sum_{q\lambda} \Delta(\vec{Q} - \vec{q}) \frac{(\vec{Q} \cdot \vec{e}_{q\lambda})^2}{\omega_{q\lambda}} A_{q\lambda}(\omega) , \quad (19)$$

where

$$A_{q\lambda}(\omega) = (n_\omega + 1) B_{q\lambda}(\omega), \quad n_\omega = (e^{\beta\hbar\omega} - 1)^{-1} \quad (20)$$

and

$$B_{q\lambda}(\omega) = \frac{8\omega_{q\lambda}^2 \Gamma_{q\lambda}(\omega)}{[\omega^2 - \omega_{q\lambda}^2 - 2\omega_{q\lambda}\Delta_{q\lambda}(\omega)]^2 + [2\omega_{q\lambda}\Gamma_{q\lambda}(\omega)]^2} . \quad (21)$$

The rigorous derivation of this equation follows from anharmonic many-body perturbation theory[33] and will not be discussed here. We state only that Δ and Γ are the shift and width (inverse lifetime) due to phonon-phonon interactions. The lowest order contribution to Γ arises from the possibility of a phonon decaying into two other phonons. The first detailed calculations for a Mie–Lennard-Jones potential that allowed for this effect were those of Bohlin and Hogberg.[27] Applications using self-consistent-phonon theory have been reported by Koehler, Goldman *et al.*, and others.[7] In Koehler's work only the lowest-order contribution to Δ and Γ are included and in our subsequent application we will label such results by $\sum_K$. Goldman *et al.*[7] included some addition contributions to Δ and Γ and in what follows calculations based upon their approximation will be labeled $\sum_{\text{GHK}}$. For details the reader is referred to the original papers.

The interference term S_{int} which describes the coupling of the one-phonon peak to the multiphonon background was discussed by Maradudin and Ambegaokar[33] and more recently by Horner[34] and Glyde.[35] The main point here is that such terms are odd in $\vec{Q}$ and will oscillate in sign (growing in magnitude) as $\vec{Q}$ increases. Since such terms necessarily vanish at a Brillouin-zone boundary we will for convenience restrict ourselves to phonons such as these and hence not have to consider S_{int} any further. Furthermore, by evaluating S_1 in both the MD calculation and the phonon case we need not consider S_2, etc. The effect of such terms can be estimated by comparing the full MD results with the one phonon ones.

B. Self-consistent phonon calculations

We present a comparison of the phonon calculations based upon Eqs. (17) and (19) with the MD results derived from Eq. (11) in Figs. 10 and 11. Although calculations are in the one phonon approximations the phonon calculation is quantum while the MD one is classical. We have, therefore, replaced the factor $(n_\omega + 1)$ occurring in Eq. (20) of the phonon calculation by the factor $kT/\hbar\omega$ while leaving the factor $B(\omega)$ fully quantum. This procedure is essentially equivalent to applying Schofield's quantum correction[23] to the classical MD calculations in order that they at least satisfy the detailed balance condition [Eq. (5)].

Figure 10 shows the zone-boundary [100] phonons for the nearest-neighbor ($n = 1$) 2048-particle system and a (12-6) potential at about one-half the melting temperature, Fig. 10(a), and the melting point, Fig. 10(b). The calculated response using self-consistent-phonon theory depends little on whether one uses Koehler's self-energy $\sum_K$ or that of Goldman *et al.*, $\sum_{\text{GHK}}$. There is fairly good agreement with the MD data at the lower temperature except that the relative intensity of the two peaks in the longitudinal response seems to be incorrect. This is likely in part due to the fact that phonon calculation is quantum, while the MD is classical. At the higher temperature there are larger discrepancies between the two calculations. Figure 11 shows this effect more clearly for the zone-boundary [100] transverse phonon of the 864-particle system [(12-6) potential with $n = 3$]. The temperature and density correspond roughly to the

melting point of the (12-6) system (actually corresponding to slightly metastable real solid argon). Here we see the rather large discrepancy between the MD predicted peak in S_1 and that obtained using self-consistent-phonon theory. The temperature is now sufficiently high that the MD results will likely be unaffected by quantum effects. Hence the discrepancy indicates a need to improve the phonon calculations, at high temperatures. To do so it will probably be necessary to explicitly include the hard-core effects as discussed by

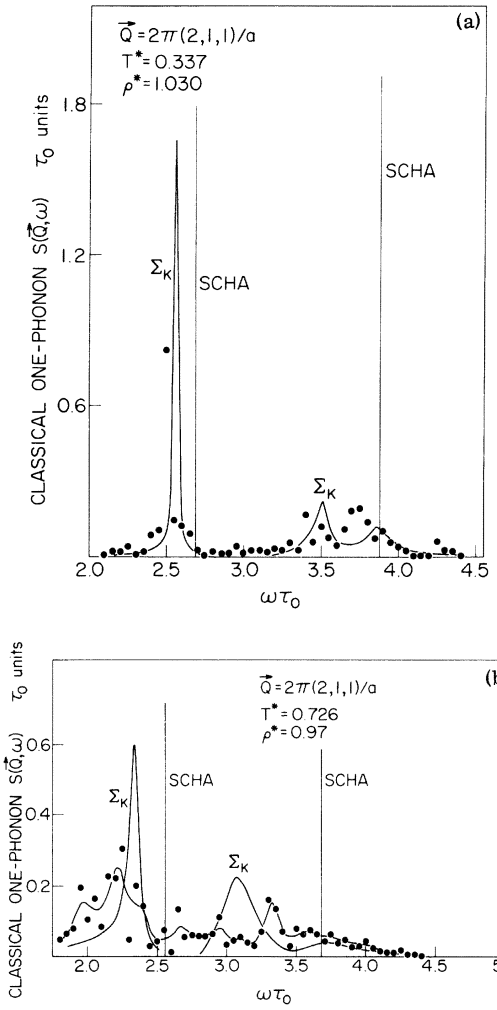

FIG. 10. (a) Detailed comparison of the one-phonon $S_1(\vec{Q},\omega)$ with the self-consistent harmonic approximation (SCHA) and anharmonic self-consistent-phonon calculations utilizing the Σ_k self-energy (see text). The dots are the unsmoothed MD data from run No. 5. (b) Detailed comparison of the one-phonon $S_1(\vec{Q},\omega)$ with the self-consistent-harmonic approximation (SCHA) and anharmonic self-consistent-phonon calculations utilizing the Σ_k self-energy (see text). The dots are the unsmoothed MD data from run No. 10. The continuous solid line through the dots is the smoothed MD data.

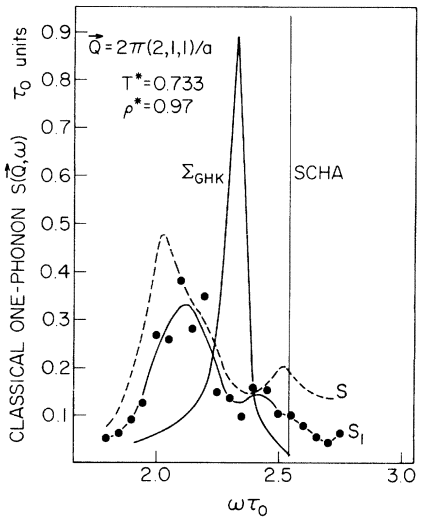

FIG. 11. Comparison of the one-phonon $S_1(\vec{Q},\omega)$ with the self-consistent-harmonic approximation (SCHA) and anharmonic self-consistent-phonon calculations utilizing the Σ_{GHK} self-energy (see text). The dots are the MD S_1 data from run No. 11 and the solid curve is the smoothed S_1 data. The dashed curve is the smoothed full $S(\vec{Q},\omega)$ which includes the multiphonon scattering.

Horner[36] and more recently by Kanney and Horton. ton.[37] Such a calculation although extremely interesting would go beyond the scope of this paper. Finally, Fig. 11 shows the full S as well as S_1 and hence indicates the extent to which multiphonon effects can distort the peak in $S(\vec{Q},\omega)$. Detailed comparisons between experiment at high temperatures and theory would necessarily involve including multiphonon effects.

VI. CONCLUSION

We have demonstrated that it is feasible to calculate the dynamical structure factor $S(\vec{Q},\omega)$ for solids using the computer simulation MD technique. Results for the (12-6) Mie–Lennard-Jones potential show many of the features recently observed in inelastic neutron scattering experiments on rare gas solids. At high temperatures, the MD results for $S_1(\vec{Q},\omega)$, the one-phonon approximation to $S(\vec{Q},\omega)$ have revealed the inadequacy of self-consistent-phonon theories that do not explicitly treat the hard-core problem.

ACKNOWLEDGMENTS

We both thank D. Levesque for his invaluable help in constructing our $S(\vec{Q},\omega)$ program and J. J. Weis for valuable discussions. The self-consistent-phonon calculations were kindly provided by V. V. Goldman. This work was completed while one of us (M. L. K) was a visitor to the Laboratoire de Physique Théorique des Liquides, Université Paris VI, under the CNRS-NRC exchange agreement.

*Laboratoire associé au Centre National de la Recherche Scientifique.
[1]B. J. Alder and T. E. Wainwright, J. Chem. Phys. 31, 459 (1959).
[2]A. Rahman, Phys. Rev. 136, A405 (1964).
[3]L. Verlet, Phys. Rev. 159, 98 (1967).
[4]N. Metropolis, A. W. Rosenbluth, M. N. Rosenbluth, A. M. Teller, and E. Teller, J. Chem. Phys. 21, 1087 (1953).
[5]See, e.g., the extensive review article by W. W. Wood, in *Physics of Simple Liquids*, edited by H. N. V. Temperley, J. S. Rowlinson, and G. S. Rushboroke (North-Holland, Amsterdam, 1968).
[6]A. C. Holt, W. G. Hoover, S. G. Gray, and D. R. Shortle, Physica (Utr.) 49, 61 (1970); M. L. Klein and W. G. Hoover, Phys. Rev. B 4, 537 (1971).
[7]T. R. Koehler, Phys. Rev. Lett. 22, 777 (1969); V. V. Goldman, G. K. Horton, and M. L. Klein, Phys. Rev. Lett. 24, 1424 (1970).
[8]J. M. Dickey and A. Paskin, Phys. Rev. 188, 1407 (1969).
[9]D. Levesque, L. Verlet, and J. Kürkijarvi, Phys. Rev. A 7, 1690 (1973).
[10]A. Rahman, Phys. Rev. Lett. 32, 52 (1974).
[11]J. P. Hansen, E. L. Pollock, and I. R. McDonald, Phys. Rev. Lett. 32, 277 (1974).
[12]J. P. Hansen and M. L. Klein, J. Phys. Lett. 35, L-29 (1974).
[13]M. L. Klein, G. Jacucci, and I. R. McDonald, J. Phys. Lett. 36, L-97 (1975); J. J. Weis and M. L. Klein, J. Chem. Phys. 63, 2869 (1975).
[14]D. N. Batchelder, B. C. G. Haywood, and D. M. Saunderson, J. Phys. C 4, 910 (1971).
[15]P. A. Fleury, J. M. Worlock, and M. L. Carter, Phys. Rev. Lett. 30, 591 (1973); H. E. Jackson, D. Landheer, and B. P. Stoicheff, *ibid.* 31, 296 (1973).
[16]B. J. Alder, H. Strauss, and J. J. Weis, J. Chem. Phys. 59, 1002 (1973).
[17]B. J. Alder, J. P. Hansen, M. L. Klein, H. Strauss, and J. J. Weis (unpublished).
[18]J. J. Weis, Molec. Phys. 28, 187 (1974).
[19]J. P. Hansen and L. Verlet, Phys. Rev. 184, 151 (1969).
[20]J. P. Hansen, Phys. Rev. A 2, 221 (1970).
[21]E. Wigner, Phys. Rev. 40, 149 (1932).
[22]J. P. Hansen and J. J. Weis, Phys. Rev. 188, 314 (1969).
[23]P. Schofield, Phys. Rev. Lett. 4, 239 (1960).
[24]J. L. Lebowitz, J. K. Percus, and L. Verlet, Phys. Rev. 153, 250 (1967).
[25]W. G. Hoover and F. H. Ree, J. Chem. Phys. 47, 4873 (1967); see also E. L. Pollock (unpublished).
[26]H. C. Andersen, J. D. Weeks, and D. Chandler, Phys. Rev. A 4, 1597 (1971); L. Verlet and J. J. Weis, *ibid.* 5, 939 (1972).
[27]L. Bohlin and T. Högberg, J. Chem. Phys. Solids 29, 1805 (1968); L. Bohlin, Solid State Commun. 9, 141 (1971); 10, 1219 (1972).
[28]J. Skalyo, Y. Endoh, and G. Shirane, Phys. Rev. B 9, 1797 (1974).
[29]Y. Fujii, N. A. Lurie, R. Pynn, and G. Shirane, Phys. Rev. B 10, 3647 (1974).
[30]V. Ambegaokar, J. Conway, and G. Baym, in *Lattice Dynamics* edited by R. F. Wallis (Pergamon, New York, 1965), p. 261.
[31]G. K. Horton, V. V. Goldman, and M. L. Klein, J. Appl. Phys. 41, 5138 (1970).
[32]F. Clayton and D. N. Batchelder, J. Phys. C 6, 1213 (1973).
[33]A. A. Maradudin and A. E. Fein, Phys. Rev. 128, 2589 (1962); A. A. Maradudin and V. Ambegaokar, *ibid.* 135, A1071 (1964).
[34]H. Horner, Phys. Rev. Lett. 29, 556 (1972).
[35]H. R. Glyde, Can. J. Phys. 52, 2281 (1974).
[36]H. Horner, Solid State Commun. 9, 79 (1971); see also Chap. 8 in *Dynamical Properties of Solids*, edited by G. K. Horton and A. A. Maradudin (North-Holland, Amsterdam, 1974).
[37]L. B. Kanney and G. K. Horton, Phys. Rev. Lett. 34, 1565 (1975).